In vivo real-time rectal wall dosimetry for prostate radiotherapy

Nicholas Hardcastle
University of Wollongong, nhardc@uow.edu.au

Dean L. Cutajar
University of Wollongong, deanc@uow.edu.au

Peter E. Metcalfe
University of Wollongong, metcalfe@uow.edu.au

Michael L F Lerch
University of Wollongong, mlerch@uow.edu.au

Vladimir L. Perevertaylo

See next page for additional authors

Authors

Nicholas Hardcastle, Dean L. Cutajar, Peter E. Metcalfe, Michael L F Lerch, Vladimir L. Perevertaylo, Wolfgang A. Tome, and Anatoly B. Rosenfeld

In vivo real-time rectal wall dosimetry for prostate radiotherapy

Nicholas Hardcastle[1,5]**, Dean L Cutajar**[1]**, Peter E Metcalfe**[1]**, Michael L F Lerch**[1]**, Vladimir L Perevertaylo**[2]**, Wolfgang A Tomé**[1,3,4] **and Anatoly B Rosenfeld**[1,6]

[1] Centre for Medical Radiation Physics, University of Wollongong, Wollongong, NSW 2522, Australia
[2] SPA BIT, Kiev, Ukraine
[3] Department of Human Oncology, University of Wisconsin–Madison, 600 Highland Ave., K4/314, Madison, WI 53792, USA
[4] Department of Medical Physics, University of Wisconsin–Madison, 600 Highland Ave., K4/314, Madison, WI 53792, USA

E-mail: anatoly@uow.edu.au

Abstract

Rectal balloons are used in external beam prostate radiotherapy to provide reproducible anatomy and rectal dose reductions. This is an investigation into the combination of a MOSFET radiation detector with a rectal balloon for real-time *in vivo* rectal wall dosimetry. The MOSFET used in the study is a radiation detector that provides a water equivalent depth of measurement of 70 μm. Two MOSFETs were combined in a face-to-face orientation. The reproducibility, sensitivity and angular dependence were measured for the dual MOSFET in a 6 MV photon beam. The dual MOSFET was combined with a rectal balloon and irradiated with hypothetical prostate treatments in a phantom. The anterior rectal wall dose was measured in real time and compared with the planning system calculated dose. The dual MOSFET showed angular dependence within $\pm 2.5\%$ in the azimuth and $+2.5\%/-4\%$ in the polar axes. When compared with an ion chamber measurement in a phantom, the dual MOSFET agreed within 2.5% for a range of radiation path lengths and incident angles. The dual MOSFET had reproducible sensitivity for fraction sizes of 2–10 Gy. For the hypothetical prostate treatments the measured anterior rectal wall dose was 2.6 and 3.2% lower than the calculated dose for 3DCRT and IMRT plans. This was expected due to limitations of the dose calculation method used at the balloon cavity interface. A dual MOSFET combined with a commercial rectal balloon was shown to provide reproducible measurements of the anterior rectal

[5] Now at Department of Human Oncology, University of Wisconsin, Madison, 600 Highland Ave., K4/314, Madison, WI 53792, USA.
[6] Author to whom any correspondence should be addressed.

wall dose in real time. The measured anterior rectal wall dose agreed with the expected dose from the treatment plan for 3DCRT and IMRT plans. The dual MOSFET could be read out in real time during the irradiation, providing the capability for real-time dose monitoring of the rectal wall dose during treatment.

(Some figures in this article are in colour only in the electronic version)

Introduction

Modern external beam radiotherapy for prostate cancer involves the delivery of high doses using highly conformal delivery techniques. Increased prostate dose has been shown to increase local control (Hanks *et al* 1998, Pollack *et al* 2000, Zelefsky *et al* 1998). Additionally, hypofractionation has been shown to be an attractive delivery method due to the apparent low alpha/beta ratio for the prostate (Brenner and Hall 1999, Brenner *et al* 2002, Fowler *et al* 2001). Increasing the total treatment dose or the dose per fraction increases the need for accurate delivery verification.

In vivo dosimetry of the rectal wall is an appealing method for verification of target and organ at risk (OAR) doses. An *in vivo* dosimeter placed on the anterior rectal wall would allow the clinician to measure the dose delivered to the section of the rectum receiving the highest dose. This is important, particularly for recent hypofractionation schedules, where high doses are delivered to the prostate and anterior rectal wall, and would be particularly useful in the context of the limitations of dose calculation algorithms at cavity interfaces (Hardcastle *et al* 2009, Keall and Hoban 1996, Martens *et al* 2002). Additionally, accurate knowledge of the anterior rectal wall dose is necessary for the correlation of the delivered dose with rectal toxicity. A secondary application of an *in vivo* anterior rectal wall dosimeter would be for target dose verification. The anterior rectal wall is generally contained by the planning target volume (PTV); therefore any dosimeter placed on the anterior rectal wall can be used as a surrogate for the PTV dose at the posterior region of the volume.

Recent articles have focused on implantable *in vivo* dosimeters for target dose verification (Beyer *et al* 2007, Black *et al* 2005, Fagerstrom *et al* 2008, Kry *et al* 2009, Scarantino *et al* 2005, 2008). This is a useful method of *in vivo* dose verification for prostate radiotherapy, with the added advantage that the implanted dosimeter can be used for position verification (Kry *et al* 2009). Other methods have focused on placing a dosimeter in a urethral catheter, for *in vivo* verification of the prostate dose in brachytherapy (Bloemen-van Gurp *et al* 2009a, 2009b, Cygler *et al* 2006, Soriani *et al* 2007). Yet another tool for *in vivo* prostate dosimetry is the electronic portal imaging device (EPID). Various studies have been presented that investigate using the EPID to measure transmitted fluence and then using this measured fluence to calculate the dose delivered to the patient. These methods are summarized by van Elmpt *et al* (2008).

This phantom study investigates another method of *in vivo* dosimetry for prostate radiotherapy using rectal balloons. Rectal balloons are used in a number of institutions in prostate radiotherapy to immobilize the prostate and reduce the amount of rectal wall irradiated to high doses (McGary *et al* 2002, Patel *et al* 2003, Teh *et al* 2002, 2005, van Lin *et al* 2005a, 2005b, 2007, Wachter *et al* 2002). Rectal balloons are placed in the rectum for each treatment fraction. Rectal balloons provide an excellent means for the placement of an *in vivo* dosimeter. In this paper, the utility of a commercial rectal balloon in combination with a MOSFET detector for real-time *in vivo* dose measurements at the rectal wall is examined.

Figure 1. MOSFET detectors placed in the outer lumen of the RadiaDyne rectal balloon.

Real-time rectal wall measurements were carried out on a specially designed phantom in conventional external beam radiotherapy scenarios.

Methods and materials

MOSFET detectors

MOSFET detectors have been used extensively for *in vivo* dosimetry (Butson *et al* 1996, Quach *et al* 2000, Scalchi and Francescon 1998, Scalchi *et al* 2005, Zilio *et al* 2006). The advantages of the MOSFET dosimetry system for point dose measurements are their relatively small size and real-time readout capabilities (Kron *et al* 2002, Rosenfeld *et al* 2001). MOSFET dosimetry relies on ionizing radiation altering the electrical properties of the MOSFET, specifically the threshold voltage (V_t), for a given source–drain current. The change in V_t is proportional to the absorbed dose. A MOSFET detector developed at the Centre of Medical Radiation Physics (CMRP) (known as the 'MO*Skin*') was used for all measurements. This specific MOSFET detector has been described in detail elsewhere and has been used extensively for *in vivo* measurements (Hardcastle *et al* 2008, Kwan *et al* 2008a, 2008b, 2009, Qi *et al* 2009). In summary, this MOSFET has a reproducible water equivalent depth (WED) of measurement of 70 μm with a sensitive volume defined by the volume of the gate oxide of 4.8×10^{-6} mm^3. This makes the design of the MOSFET ideal for dosimetry in high dose gradient regions, such as the rectal wall in the presence of a rectal balloon air cavity.

In the case of measurements at depth (rather than at the surface), two MOSFETs are used, in a face-to-face arrangement. This face-to-face dual MOSFET arrangement is referred to in the remainder of this text as the 'dual MOSFET'. The dual MOSFET, proposed and developed at CMRP, allows for angular-independent measurements as it negates the naturally asymmetrical structure of the MOSFET chip relative to the beam direction (Rosenfeld *et al* 2005). It must be stated that this definition of the dual MOSFET is functionally different to commercial dual MOSFET detectors, where two MOSFET chips on the same Si substrate are used for temperature compensation (Soubra *et al* 1994). In our case, the dual MOSFET relates to correction of angular anisotropy and not temperature compensation. The dual MOSFET results in a dose measurement effectively made over a 140 μm thick region. The dual MOSFET was embedded into the outer lumen of a commercial rectal balloon (RadiaDyne, Houston TX, USA), as shown in figure 1, such that it was fully contained within the balloon.

Table 1. MOSFET sensitivity for varying fraction sizes.

Fraction Size (cGy)	Dose per 'beam' (cGy)	Sensitivity (mV cGy^{-1})
203	29	2.63
252	36	2.63
301	43	2.65
350	50	2.65
497	71	2.63
749	107	2.61
1001	143	2.62
	Average ($\pm$SD)	2.63 $\pm$ 0.01

The MOSFET detectors are read out in real time using an in-house developed reader. The reader provides a 15 V gate voltage to the MOSFET during irradiation. The reader then supplies a constant source–drain current to deduce V_t. The reader can be used to readout V_t manually or can be controlled by a PC for automatic readout over a given time interval at a set frequency using in-house developed software (Rosenfeld *et al* 2001).

Reproducibility and sensitivity

The reproducibility of the sensitivity of the MOSFET detector, that is the change in V_t for irradiation to known doses, was measured. The sensitivity was investigated for a range of simulated treatment fraction deliveries from 2 to 10 Gy/fraction, including simulated breaks for gantry motion between beams. The rectal balloons are designed for one fraction use only; each balloon/MOSFET would receive only one fraction of the dose. The MOSFETs were irradiated at 1.5 cm depth in a $30 \times 30 \times 11.5$ cm^3 water slab with a 10×10 cm^2 6 MV photon beam at a 100 cm SSD. Seven field treatment fractions of 2–10 Gy/fraction were simulated by irradiating a MOSFET up to the fraction dose in seven equal increments (to simulate irradiation from each 'beam'). A delay of 30 s was used between each 'beam' to simulate gantry rotation time between beams. A new MOSFET with no dose history was used for each simulated fraction. The fraction sizes simulated are given in table 1.

Angular dependence

The angular dependence of the dual MOSFET configuration was measured on two axes in a 6 MV photon beam from a Varian 21EX Linac. The angular dependence in the azimuth axis was measured by placing the dual MOSFET in a cylindrical phantom that was embedded in a square, solid water phantom at a depth of 5 cm. The dual MOSFET was then irradiated from a beam incident every 30° for a full rotation. This was repeated twice. The cylinder containing the dual MOSFET was rotated, rather than the Linac gantry, to maintain a constant radiation path length to the location of the detector. The polar angular dependence was measured by placing the dual MOSFET in the centre of a 10 cm diameter cylinder, orthogonal to the cylinder's longitudinal axis. The dual MOSFET was irradiated with a 5×5 cm^2 field in increments of 30° around the full 360° of the cylinder. For each measurement, the average response of the two detectors was then taken as the final reading. All readings were normalized to the average of the measurements at each angle for each measurement axis.

A further set of measurements with the dual MOSFET was performed to measure the angular dependence at different depths using a clinical IMRT verification phantom (I'mRT,
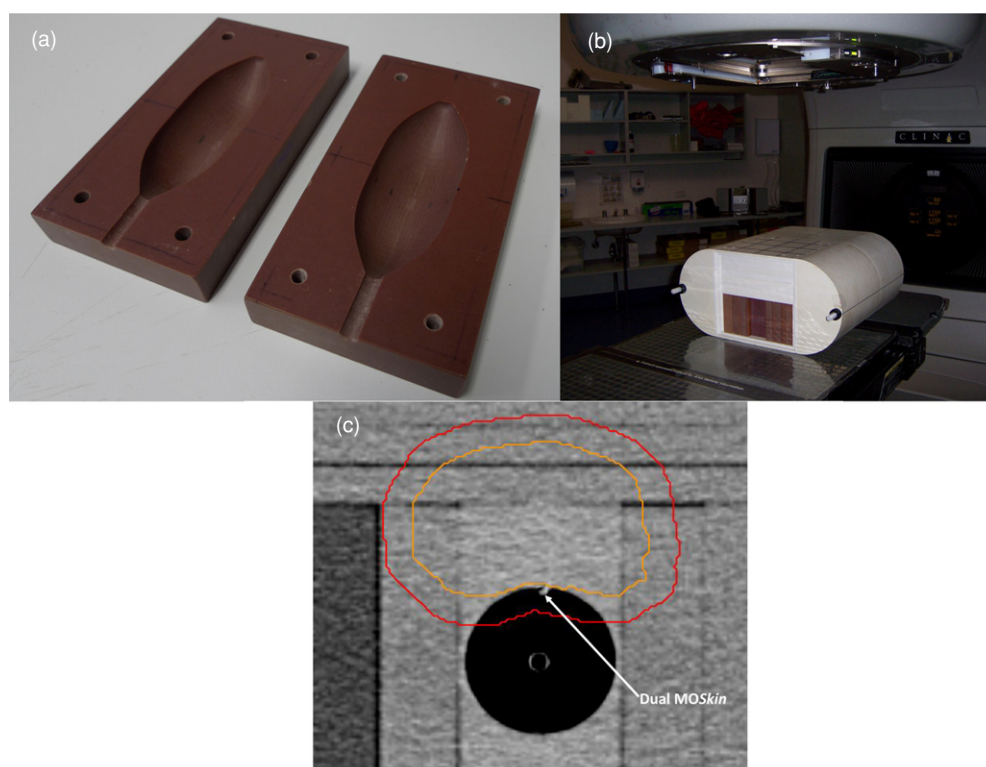
Figure 2. (a) Custom-made phantom to house the rectal balloon, (b) balloon phantom placed inside the IMRT phantom and (c) CT slice of the phantom showing the dual MOSFET location relative to the hypothetical prostate (inner contour) and PTV (outer contour).

IBA Dosimetry, Germany). The dual MOSFET was placed at the centre of the phantom and calibrated. Calibration was performed by irradiating the dual MOSFET with a known dose and recording the response of both detectors. The dual MOSFET was then flipped and the calibration was repeated. For each calibration measurement the change in threshold voltage for each detector was added. The average of the responses (i.e. in both orientations) was then divided by the known dose (100 cGy) to give the MOSFET sensitivity in mV cGy^{-1}. The calibration coefficient is the inverse of the sensitivity and has the units of cGy mV^{-1}. The voltage reading is multiplied by the calibration coefficient to obtain the dose.

The dual MOSFET was then irradiated with gantry angles every 45° for the full 360° (detector was at the machine isocentre). Each measurement was multiplied by the dual MOSFET calibration coefficient to result in an absolute dose for each measurement. The dual MOSFET was then replaced with an ion chamber. The ion chamber was calibrated by irradiating with a known dose. The ion chamber was then irradiated with the same gantry angles as the dual MOSFET. The dual MOSFET dose was normalized to the ion chamber measurement at each angle. All measurements were repeated twice.

Treatment simulation measurements

A custom-made phantom was built to match the external contours of the balloon. This phantom was placed in the IMRT phantom. The phantom setup is shown in figure 2. A planning CT scan was taken of the phantom setup. The CT data were transferred into the Pinnacle RTPS (Philips

Healthcare, Fitchburg, WI, USA) where the contours of a hypothetical prostate, rectum (the balloon cavity), bladder and femoral heads were created. Seven field 3DCRT and IMRT plans were created in the Pinnacle RTPS, delivering 78 Gy in 2 Gy fractions to the isocentre of a hypothetical prostate target in the phantom. The MOSFET was visible on the CT scan (figure 2(c)) and the planned dose to the MOSFET was recorded for both treatment plans. Three fractions each of the 3DCRT and IMRT plans were then delivered to the phantom.

The dose delivered to the dual MOSFET was recorded at a frequency of 1 Hz during each delivery by connecting the reader to a PC, and using in-house developed software. The dual MOSFET was irradiated in an active mode, meaning a bias voltage was applied to the gate oxide during irradiation to increase sensitivity. During readout, the gate voltage was inverted and the threshold voltage was obtained for a given readout current. As the gate voltage of the MOSFET was inverted during this readout, the charge collection in the active volume, and hence the sensitivity, was affected. However, the readout of the MOSFET, controlled by a microprocessor, took approximately 100 μs or 0.01% of the duty cycle, meaning this effect was negligible.

Results

Reproducibility

The sensitivity of seven MOSFET detectors from the same batch for irradiation for fraction sizes of 2–10 Gy (each 'fraction' irradiated in seven increments) is presented in table 1. The response of the seven MOSFET detectors was on average (±standard deviation) 2.63 ± 0.01 mV cGy^{-1}.
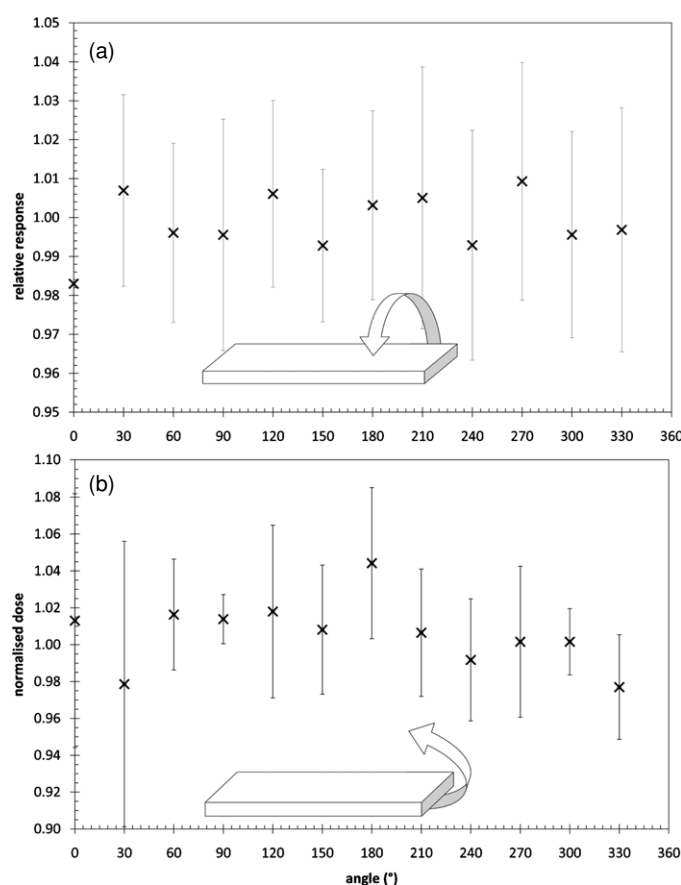
Angular dependence

The angular dependence of the dual MOSFET is presented in figure 3. The results are the average of three measurements and the error bars are two standard deviations of the mean. The variation in the readings for the azimuth axis was within ±2.5%. For the polar axis the readings were between −2.5% and +4% of the average of all readings.

The dual MOSFET measured dose, relative to the ion chamber measurement at the centre of the IMRT phantom for beams incident from various angles is given in figure 4. The dual MOSFET measured dose at the centre of the IMRT phantom was within ±2.5% of the ion chamber measured dose at the same location.

Treatment simulation measurements

The dual MOSFET real-time measured dose, at the anterior rectal wall in a phantom setup, is presented in figure 5. The error bars are the 95% confidence interval of the average of three measurements. For the 3DCRT plan, the dual MOSFET measured dose was 184.5 ± 0.8 cGy and the RTPS calculated dose was 189.4 cGy. This is a difference of −5.1 cGy, or the dual MOSFET measured dose is 2.6% lower than the planned dose. For the IMRT plan, the influence of the segmented dose delivery is apparent in the more jagged shape of the real-time dose accrual plot. The dual MOSFET measured dose was 185.1 ± 1.3 cGy and the RTPS calculated dose was 191.2 cGy. This is a difference of 6.1 cGy, or the dual MOSFET measured dose is 3.2% lower than the planned dose.

The RTPS calculated dose for each field was compared with the dual MOSFET measured dose for each field for the 3DCRT and IMRT treatment deliveries. Figure 6 shows the comparison between the planned and measured rectal wall dose. For the 3DCRT plan, the

Figure 3. Angular dependence of the dual MOSFET detector for (a) azimuth and (b) polar axes. The error bars represent two standard deviations of the mean of three measurements.

dual MOSFET measured doses agree, within error limits, with the RTPS calculated dose for the 120, 40, 0 and 320° beams. For the 80, 240 and 280° beams, the RTPS is 1.0, 1.4 and 3.2 cGy more than the dual MOSFET measured dose, respectively. For the IMRT plan, the dual MOSFET measured doses agree within error limits with the RTPS calculated dose for the 40, 0 and 320° beams. For the 120, 80, 240 and 280° beams, the RTPS calculated dose is 2.3, 1.5, 0.7 and 1.25 cGy greater than the dual MOSFET measured doses, respectively.

Discussion

This study presents the initial results from the testing of a MOSFET dosimeter developed at the CMRP combined with a rectal balloon for use in real-time *in vivo* dosimetry. In this phantom study, the performance of a dual MOSFET configuration in combination with a commercial rectal balloon was investigated to determine the utility of this apparatus for clinical use.

The MOSFET detectors showed a reproducible sensitivity for fraction sizes of 2–10 Gy. The very good reproducibility of the MOSFET sensitivity (within 1%) is related to the low dose exposures up to 10 Gy, where there is limited radiation damage to the SiO–Si interface. Thus, the instability of the MOSFET reading is limited. In addition, this comparison was only performed for MOSFETs from the same manufacturing batch. For higher doses, the
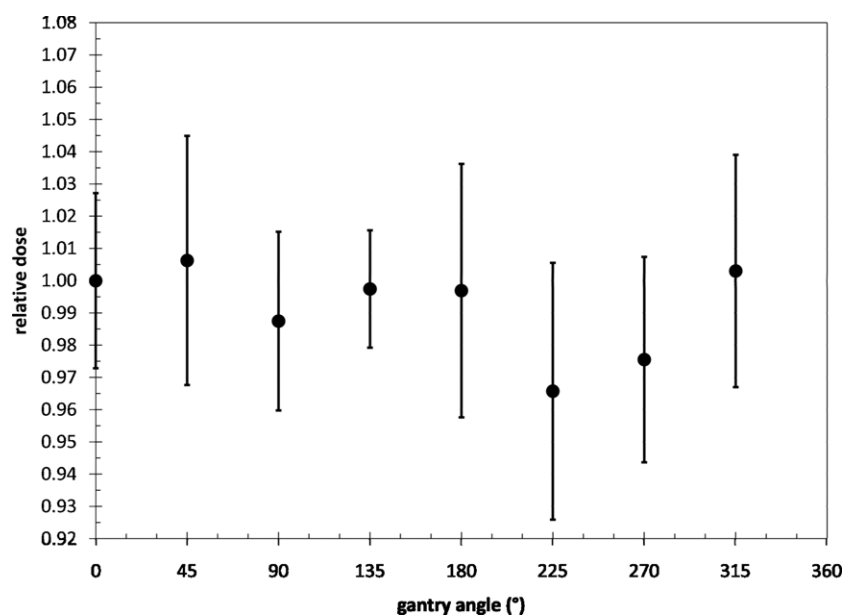
Figure 4. Dual MOSFET dose relative to the ion chamber measured dose at the centre of the IMRT phantom for a range of beam angles. The error bars are two standard deviations of the average of three measurements.

reproducibility of the sensitivity of MOSFETs is approximately 2% and should be investigated in the future for multiple batches of these particular MOSFETs. This MOSFET is thus suitable for *in vivo* real-time dose monitoring in hypofractionation schedules of up to 10 Gy/fraction, such as those seen in prostate cancer radiotherapy. Although the lifetime of the MOSFET is limited to approximately 50 Gy, commercial rectal balloons are designed for one-time use only; therefore it is expected that both the balloon and the MOSFET will be discarded after each fraction has been delivered, which for prostate radiotherapy would typically be less than 10 Gy.

The dual MOSFET has an angular dependence of $\pm 2.5\%$ from all incident beam angles. Therefore, it can be used in rotational therapies such as tomotherapy and volumetric modulated arc therapy (VMAT) without the need for angular correction.

When placed on the anterior wall of a commercial rectal balloon and irradiated with clinical 3DCRT and IMRT plans, the dual MOSFET provided a real-time dose measurement of the anterior rectal wall dose. The anterior rectal wall dose was measured to be 2.6 and 3.2% lower than the RTPS calculation for the 3DCRT and IMRT plans, respectively. Previous studies have shown that the collapsed cone convolution/superposition dose calculation algorithm used in this study over-predicts the anterior rectal wall dose when an air-filled rectal balloon is used (Hardcastle *et al* 2009). Therefore the lower measured dose, relative to the RTPS calculation, concurs with this previous finding.

In figure 6 it is shown that the dual MOSFET measured doses agree with the RTPS calculated doses for the 320, 0 and 40° beams for both the 3DCRT and IMRT cases. The RTPS calculated doses were greater than the dual MOSFET measured doses for the 120 (IMRT only), 80, 280 and 240° beams. These beams deliver doses to the target from beam angles that are more tangential to the target with respect to the balloon cavity. Although the absolute value of the differences was small, this agrees with a previous study which showed that the greatest discrepancy between the RTPS calculated dose and the measured dose, at the anterior rectal
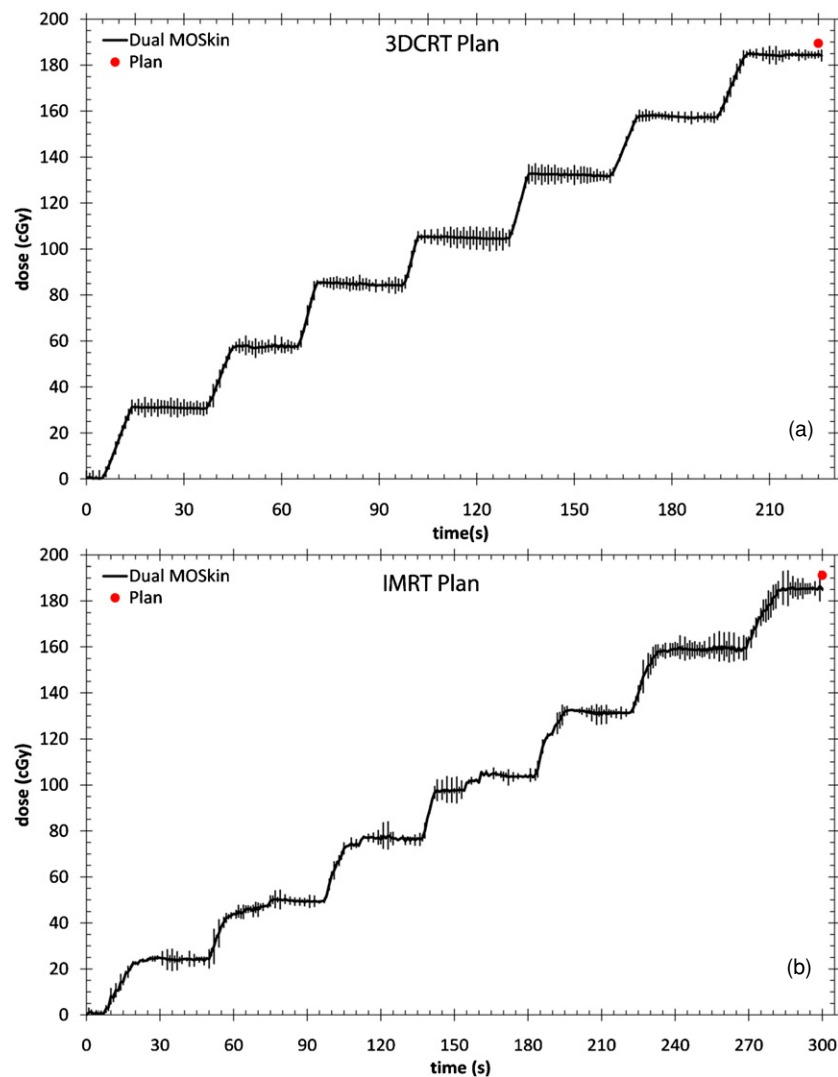
Figure 5. Real-time measured anterior rectal wall dose for (a) the 3DCRT plan and (b) the IMRT plan. The error bars are the 95% confidence interval of the average of three measurements.

wall in the presence of a rectal balloon cavity, was when the beams were incident laterally to the target, with respect to the cavity (Hardcastle *et al* 2009). This is due to limitations in the convolution/superposition dose calculation where lateral electron disequilibrium exists. Therefore any differences between the RTPS calculated and measured doses at the anterior rectal wall when an air-filled rectal balloon is used would be expected to be due mainly to the contribution from lateral beams.

The MOSFET could be read out at 1 Hz during the delivery of a radiotherapy treatment fraction. The ability to read out the MOSFET in real time allows the rectal dose to be tracked as it is being delivered, potentially providing a 'dose alarm' if the rectal wall dose exceeds a set tolerance. This has been shown in the results in figure 6; the tracking of the anterior rectal wall dose can be performed on a field-by-field basis. Although the rectal balloon reduces prostate motion significantly, rectal motion can still occur which may increase the rectal wall
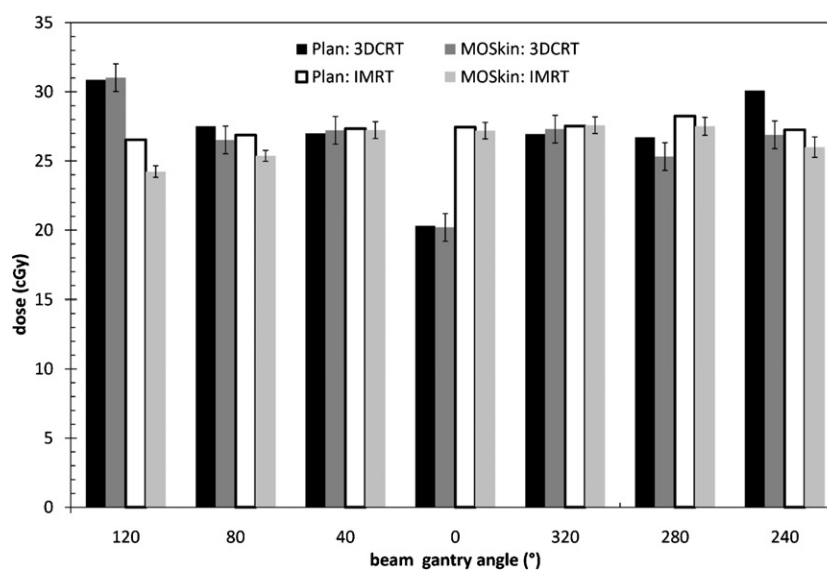
Figure 6. A field-by-field comparison of the RTPS calculated and MOSFET measured anterior rectal wall dose for the 3DCRT and IMRT deliveries.

dose. Conversely, if the rectal wall dose is significantly lower than the expected dose this could mean part of the PTV is being underdosed. At the very least, this *in vivo* dosimetry system provides tracking and verification of daily delivered rectal wall doses, which may prove useful in the case of observed enhancement of toxicity or local recurrence. The correlation of rectal toxicity rates with the absorbed dose currently relies on the calculated dose at the time of planning. This device would provide a direct measurement of the anterior rectal wall dose for each treatment fraction, increasing the accuracy of toxicity correlation.

The use of this *in vivo* detector system will become more complicated when used in clinical patients. Complications may arise due to temperature changes of the MOSFET during irradiation and balloon positioning in the patient. These complications must be taken into account to ensure accurate dosimetry.

The threshold voltage of the MOSFET detectors is sensitive to temperature variations unless the readout current corresponds to the thermostable current, as used in the current reader. The thermostable current is the readout current (source–drain current) at which the threshold voltage is constant for varying temperature. The thermostable current is constant for the dose range presented in this paper. The sensitivity of the MOSFET detector to radiation is temperature independent within the (15–40°) range (Cheung 2004). Thus calibration made at any room temperature, if held constant during the calibration process, will be valid for irradiation at different temperatures, for example 37° on a patient's body, assuming that the MOSFET temperature is constant during real-time dosimetry. However, the threshold voltage of the MOSFET changes with temperature (Cheung 2004). Therefore, In order to avoid temperature errors associated with transition time where the MOSFET detector is placed on the patient's body, but does not have enough time to obtain thermal equilibrium before measurements commence, the threshold voltage reading of the MOSFET detector should be temperature independent or compensated for. This has been achieved in other MOSFET detection systems using a dual MOSFET with different gate bias during irradiation (Soubra *et al* 1994). The next-generation CMRP readout system for MOSFET and dual MOSFET detectors is temperature independent for any readout current without requiring an additional

MOSFET chip. This system utilizes the intrinsic properties of MOSFET detectors for real-time correction of temperature changes without the need for additional temperature sensors (Rozenfeld 2008).

A second complication arises in balloon/detector positioning. Currently the balloon has markings on the stem which help to ensure the correct depth of insertion during simulation and delivery of the treatment. During the treatment, detector localization accuracy would depend on the level of image guidance being employed. As shown in figure 2(c), the MOSFET is visible on the planning CT. Therefore, kilovoltage CT image data taken immediately prior to treatment delivery would provide accurate detector location for this snapshot of time. In this case, the dose could be recalculated to obtain the expected daily dose for comparison with the measured dose, integrating with any image guidance or adaptive protocols. If this level of image guidance were not employed, then the MOSFET location would not be known as accurately in the face of anatomical changes. In the case of variation in balloon positioning between fractions, a future design could employ multiple dual MOSFET detectors placed in a strip along the superior–inferior axis of the balloon. This would provide dose measurements at multiple locations along the anterior rectal wall relative to the PTV and improve the probability of measurement of the highest anterior rectal wall dose. In addition to anterior rectal wall dose measurements, MOSFET detectors could be placed at other locations around the balloon, such as the posterior side, to obtain more absorbed dose to the rectum data.

Conclusion

A real-time *in vivo* dosimetry system for tracking of rectal wall doses in prostate radiotherapy has been presented. The dosimetry system provides real-time tracking of the rectal wall dose during the delivery of a treatment fraction. The MOSFET detectors provided reproducible, angular-independent dose measurements and linear responses for fraction sizes of 2–10 Gy. A dual MOSFET configuration was used in a phantom setup to measure in real time the anterior rectal wall dose for 3DCRT and IMRT treatments (delivering 2 Gy/fraction). The measured anterior rectal wall doses were in close agreement with the RTPS calculation and consistent with previous dosimetry studies in this situation.

Acknowledgments

References

Beyer G P, Scarantino C W, Prestidge B R, Sadeghi A G, Anscher M S, Miften M, Carrea T B, Sims M and Black R D 2007 Technical evaluation of radiation dose delivered in prostate cancer patients as measured by an implantable MOSFET dosimeter *Int. J. Radiat. Oncol. Biol. Phys.* **69** 925–35

Black R D, Scarantino C W, Mann G G, Anscher M S, Ornitz R D and Nelms B E 2005 An analysis of an implantable dosimeter system for external beam therapy *Int. J. Radiat. Oncol. Biol. Phys.* **63** 290–300

Bloemen-Van Gurp E J, Haanstra B K C, Murrer L H P, Van Gils F C J M, Dekker A L A J, Mijnheer B J and Lambin P 2009a *In vivo* dosimetry with a linear MOSFET array to evaluate the urethra dose during permanent implant brachytherapy using iodine-125 *Int. J. Radiat. Oncol. Biol. Phys.* **75** 1266–72

Bloemen-Van Gurp E J, Murrer L H P, Haanstra B K C, Van Gils F C J M, Dekker A L A J, Mijnheer B J and Lambin P 2009b *In vivo* dosimetry using a linear Mosfet-array dosimeter to determine the urethra dose in 125I permanent prostate implants *Int. J. Radiat. Oncol. Biol. Phys.* **73** 314–21

Brenner D J and Hall E J 1999 Fractionation and protraction for radiotherapy of prostate carcinoma *Int. J. Radiat. Oncol. Biol. Phys.* **43** 1095–101

Brenner D J, Martinez A A, Edmundson G K, Mitchell C, Thames H D and Armour E P 2002 Direct evidence that prostate tumors show high sensitivity to fractionation (low alpha/beta ratio), similar to late-responding normal tissue *Int. J. Radiat. Oncol. Biol. Phys* **52** 6–13

Butson M J, Rozenfeld A, Mathur J N, Carolan M, Wong T P Y and Metcalfe P E 1996 A new radiotherapy surface dose detector: the MOSFET *Med. Phys.* **23** 655–8

Cheung T, Butson M J and Yu P K 2004 Effects of temperature variation on MOSFET dosimetry *Phys. Med. Biol.* **49** N191–6

Cygler J E, Saoudi A, Perry G, Morash C and Choan E 2006 Feasibility study of using MOSFET detectors for *in vivo* dosimetry during permanent low-dose-rate prostate implants *Radiother. Oncol.* **80** 296–301

Fagerstrom J M, Micka J A and Dewerd L A 2008 Response of an implantable MOSFET dosimeter to Ir-192 HDR radiation *Med. Phys.* **35** 5729–37

Fowler J, Chappell R and Ritter M 2001 Is alpha/beta for prostate tumors really low? *Int. J. Radiat. Oncol. Biol. Phys.* **50** 1021–31

Hanks G E, Hanlon A L, Schultheiss T E, Pinover W H, Movsas B, Epstein B E and Hunt M A 1998 Dose escalation with 3D conformal treatment: five year outcomes, treatment optimization, and future directions *Int. J. Radiat. Oncol. Biol. Phys.* **41** 501–10

Hardcastle N, Metcalfe P E, Rosenfeld A B and Tome W A 2009 Endo-rectal balloon cavity dosimetry in a phantom: performance under IMRT and helical tomotherapy beams *Radiother. Oncol.* **92** 48–56

Hardcastle N, Soisson E, Metcalfe P, Rosenfeld A B and Tome W A 2008 Dosimetric verification of helical tomotherapy for total scalp irradiation *Med. Phys.* **35** 5061–8

Keall P J and Hoban P W 1996 Superposition dose calculation incorporating Monte Carlo generated electron track kernels *Med. Phys.* **23** 479–85

Kron T, Rosenfeld A, Lerch M and Bazley S 2002 Measurements in radiotherapy beams using on-line MOSFET detectors *Radiat. Prot. Dosim.* **101** 445–8

Kry S F, Price M, Wang Z, Mourtada F and Salehpour M 2009 Investigation into the use of a MOSFET dosimeter as an implantable fiducial marker *J. Appl. Clin. Med. Phys.* **10** 22–32

Kwan I S, Lee B, Yoo A J, Cho D, Jang K, Shin S, Carolan M, Lerch M, Perevertaylo V L and Rosenfeld A B 2008a Comparison of the new MOSkin detector and fiber optic dosimetry system for radiotherapy *J. Nucl. Sci. Technol.* **S5** 518–21

Kwan I S *et al* 2008b Skin dosimetry with new MOSFET detectors *Radiat. Meas.* **43** 929–32

Kwan I S, Wilkinson D, Cutajar D, Lerch M, Rosenfeld A, Howie A, Bucci J, Chin Y and Perevertaylo V L 2009 The effect of rectal heterogeneity on wall dose in high dose rate brachytherapy *Med. Phys.* **36** 224–32

Martens C, Reynaert N, De Wagter C, Nilsson P, Coghe M, Palmans H, Thierens H and De Neve W 2002 Underdosage of the upper-airway mucosa for small fields as used in intensity-modulated radiation therapy: a comparison between radiochromic film measurements, Monte Carlo simulations, and collapsed cone convolution calculations *Med. Phys.* **29** 1528–35

Mcgary J E, Teh B S, Butler E B and Grant W 3rd 2002 Prostate immobilization using a rectal balloon *J. Appl. Clin. Med. Phys.* **3** 6–11

Patel R R, Orton N, Tome W A, Chappell R and Ritter M A 2003 Rectal dose sparing with a balloon catheter and ultrasound localization in conformal radiation therapy for prostate cancer *Radiother. Oncol.* **67** 285–94

Pollack A, Zagars G K, Smith L G, Lee J J, Von Eschenbach A C, Antolak J A, Starkschall G and Rosen I 2000 Preliminary results of a randomized radiotherapy dose-escalation study comparing 70 Gy with 78 Gy for prostate cancer *J. Clin. Oncol.* **18** 3904–11

Qi Z-Y *et al* 2009 *In vivo* verification of superficial dose for head and neck treatments using intensity-modulated techniques *Med. Phys.* **36** 59–70

Quach K Y, Morales J, Butson M J, Rosenfeld A B and Metcalfe P E 2000 Measurement of radiotherapy x-ray skin dose on a chest wall phantom *Med. Phys.* **27** 1676–80

Rozenfeld A B 2008 Radiation sensor and dosimeter *Patent* PCT/AU2008/000788, WO 2008/148150 A1

Rosenfeld A B, Lerch M L F, Kron T, Brauer-Krisch E, Bravin A and Holmes-Siedle A 2001 Feasibility study of on-line, high spatial resolution MOSFET dosimetry in static and pulsed x-ray radiation fields *IEEE Trans. Nucl. Sci.* **NS-48** 2061–8

Rosenfeld A B *et al* 2005 Edge-on face-to-face MOSFET for synchrotron microbeam dosimetry: MC modeling *IEEE Trans. Nucl. Sci.* **NS-52** 2562–9

Scalchi P and Francescon P 1998 Calibration of a mosfet detection system for 6-MV *in vivo* dosimetry *Int. J. Radiat. Oncol. Biol. Phys.* **40** 987–93

Scalchi P, Francescon P and Rajaguru P 2005 Characterization of a new MOSFET detector configuration for *in vivo* skin dosimetry *Med. Phys.* **32** 1571–8

Scarantino C W, Prestidge B R, Anscher M S, Ferree C R, Kearns W T, Black R D, Bolick N G and Beyer G P 2008 The observed variance between predicted and measured radiation dose in breast and prostate patients utilizing an *in vivo* dosimeter *Int. J. Radiat. Oncol. Biol. Phys.* **72** 597–604

Scarantino C W, Rini C J, Aquino M, Carrea T B, Ornitz R D, Anscher M S and Black R D 2005 Initial clinical results of an *in vivo* dosimeter during external beam radiation therapy *Int. J. Radiat. Oncol. Biol. Phys.* **62** 606–13

Soriani A, Landoni V, Marzi S, Laccarino G, Saracino B, Arcangeli G and Benassi M 2007 Setup verification and in vivo dosimetry during intraoperative radiation therapy (IORT) for prostate cancer *Med. Phys.* **34** 3205–10

Soubra M, Cygler J and Mackay G 1994 Evaluation of a dual bias dual metal oxide-silicon semiconductor field effect transistor detector as radiation dosimeter *Med. Phys.* **21** 567–72

Teh B S, Dong L, Mcgary J E, Mai W Y, Grant W 3rd and Butler E B 2005 Rectal wall sparing by dosimetric effect of rectal balloon used during intensity-modulated radiation therapy (IMRT) for prostate cancer *Med. Dosim.* **30** 25–30

Teh B S, Mcgary J E, Dong L, Mai W Y, Carpenter L S, Lu H H, Chiu J K, Woo S Y, Grant W H and Butler E B 2002 The use of rectal balloon during the delivery of intensity modulated radiotherapy (IMRT) for prostate cancer: more than just a prostate gland immobilization device? *Cancer J* **8** 476–83

van Elmpt W, McDermott L, Nijsten S, Wendling M, Lambin P and Mijnheer B 2008 A literature review of electronic portal imaging for radiotherapy dosimetry *Radiother. Oncol.* **88** 289–309

Van Lin E N, Hoffmann A L, Van Kollenburg P, Leer J W and Visser A G 2005a Rectal wall sparing effect of three different endorectal balloons in 3D conformal and IMRT prostate radiotherapy *Int. J. Radiat. Oncol. Biol. Phys.* **63** 565–76

Van Lin E N, Kristinsson J, Philippens M E, De Jong D J, Van Der Vight L P, Kaanders J H, Leer J W and Visser A G 2007 Reduced late rectal mucosal changes after prostate three-dimensional conformal radiotherapy with endorectal balloon as observed in repeated endoscopy *Int. J. Radiat. Oncol. Biol. Phys.* **67** 799–811

Van Lin E N, Van Der Vight L P, Witjes J A, Huisman H J, Leer J W and Visser A G 2005b The effect of an endorectal balloon and off-line correction on the interfraction systematic and random prostate position variations: a comparative study *Int. J. Radiat. Oncol. Biol. Phys.* **61** 278–88

Wachter S, Gerstner N, Dorner D, Goldner G, Colotto A, Wambersie A and Potter R 2002 The influence of a rectal balloon tube as internal immobilization device on variations of volumes and dose-volume histograms during treatment course of conformal radiotherapy for prostate cancer *Int. J. Radiat. Oncol. Biol. Phys.* **52** 91–100

Zelefsky M J, Leibel S A, Gaudin P B, Kutcher G J, Fleshner N E, Venkatramen E S, Reuter V E, Fair W R, Ling C C and Fuks Z 1998 Dose escalation with three-dimensional conformal radiation therapy affects the outcome in prostate cancer *Int. J. Radiat. Oncol. Biol. Phys.* **41** 491–500

Zilio V, Joneja O, Popowski Y, Rosenfeld A and Chawla R 2006 Calibration of MOSFET detectors for absolute dosimetry with an (IR)-I-192 HDR brachytherapy source *10th Annual Meeting of the Scientific-Association-of-Swiss-Radiation-Oncology (Sion, Switzerland)* p 175